 doi:10.20944/preprints202205.0232.v1

Article

Fatigue factor assessment and life prediction of concrete based on Bayesian regularized BP neural network

Huating Chen [1,*], Zhenyu Sun [1], Zefeng Zhong [2] and Yan Huang [1,*]

[1] Faculty of Urban Construction, Beijing University of Technology, Beijing 100124, China; chenhuating@bjut.edu.cn
[2] Baobida IOT Technology (Suzhou) Co., Ltd, 200041, China; zhongzefengwy@163.com
* Correspondence: chenhuating@bjut.edu.cn; Tel.: +86-13301137705 (H.C.) and hybridge@bjut.edu.cn (Y.H.)

Abstract: The fatigue life of concrete is affected by many interwoven factors whose effect is nonlinear. Because of its unique self-learning ability and strong generalization capability, the Bayesian regularized backpropagation neural network (BR-BPNN) is proposed to predict concrete behavior in tensile fatigue. The optimal model was determined through various combinations of network parameters. The average relative impact value (ARIV) was constructed to evaluate the correlation between fatigue life and its influencing parameters (maximum stress level Smax, stress ratio R, static strength f, failure probability P). ARIV results were also compared with other factor assessment methods (weight equation and multiple linear regression analyses). Using BR-BPNN, S-N curves were then obtained for the combinations of R=0.1, 0.2, 0.5; f=5, 6, 7MPa; P=5%, 50%, 95%. The tensile fatigue results under different testing conditions were finally compared for compatibility. It was concluded that Smax has the most significant negative effect on fatigue life; the degree of influence of R, P, and *f*, which positively correlate with fatigue life, decreases successively. ARIV is confirmed as a feasible way to analyze the importance of parameters and could be recommended for future applications. The tensile fatigue performance of plain concrete under different stress states (flexural tension, axial tension, splitting tension) does not differ significantly. Besides utilizing the valuable fatigue test data scattered in the literature, insights gained from this work could provide a reference for subsequent fatigue test program design and fatigue evaluation.

Keywords: concrete tensile fatigue; neural networks; Bayesian regularization; parameter assessment; fatigue life prediction

1. Introduction

Fatigue life is an essential indicator of fatigue performance. As a complex multiphase composite material, concrete exhibits significant discreteness in fatigue life [1]. Moreover, since a nonlinear mapping relationship exists between fatigue life and its influencing factors [2], fatigue life estimation has become the emphasis of concrete fatigue research.

The conventional method of analyzing fatigue life is based on mathematical statistics and fits experimental fatigue data to a specific regression equation. Parameters considered in the fatigue life equations initially contained only the stress level. Later, the stress ratio R [3], the failure probability P [4], and the loading frequency [5] were gradually integrated for practical applications. Despite their extensiveness and complexity, proposed equations cannot be applied to all fatigue analyses and are difficult to ensure accuracy [6]. Backpropagation neural network (BPNN), which is automatically approximated from the training data, does not need to make assumptions about the functional form [7]; it is thus feasible to improve the applicability and prediction accuracy for multi-parameter fatigue life fitting.

Although BPNN has primarily been used to predict concrete strength and durability properties, a few studies [8-11] on fatigue life prediction of concrete did demonstrate

Preprints (www.preprints.org) | NOT PEER-REVIEWED | Posted: 17 May 2022 doi:10.20944/preprints202205.0232.v1

its rationality and effectiveness. Fatigue life prediction generally approaches more accurately to the experimental results, and the model performs statistically better than the code equations [11]. BPNN prediction is affected by the mapping relationship between input and output. For example, Mohanty et al. [12] found that a three-input parameter model's predicted fatigue crack growth rate correlates better with test results than a two-input parameter one. However, these studies lacked mathematical analysis on selecting input parameters, nor is there a consensus on what are the key parameters.

BPNN for fatigue life prediction selects training data and then makes predictions for the same experiments, which fails to demonstrate generalization capability for unknown data. The learning process of the BPNN algorithm strongly depends on the training data, and its extrapolation capability is not guaranteed if a significant difference exists between the training set and the test set [13]. As illustrated in Figure 1, data is divided into a training set, test set, and validation set. It is quite possible that the trained model approximates test set or validation set data well but shows a poor prediction for an unknown data set B. This phenomenon is called overfitting. Maybe for the same reason, previous studies focused on fatigue under a particular loading condition; the relationship between concrete fatigue lives under different stress states has not been thoroughly investigated.

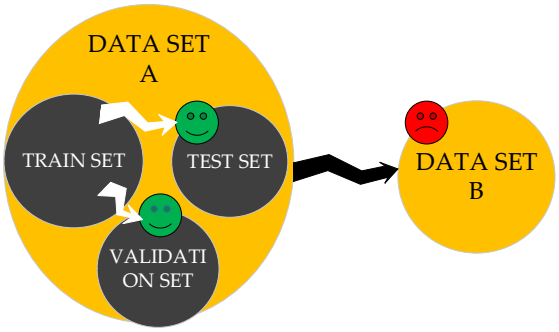

Figure 1. Sketch of poor extrapolation of the predictive model.

The regularization technique using an additional weight attenuation term in the error function in BPNN can appropriately fix the overfitting problem [14]. Bezazi et al. [14] combined BPNN with the Bayesian technique to predict fatigue probability life, and the results showed that Bayesian training could obtain better data fitting performance. The so-constructed model is a Bayesian regularized backpropagation neural network (BR-BPNN).

In order to evaluate the significance of input parameters, Garson [15] and Li et al. [16] analyzed the influence weight of each input variable based on the weight matrix, which could be applied to the single and double hidden layer neural network, respectively. Lopes et al. [17] took the contribution factor as a guide for screening input variables, calculated by the sum of the weights connected to an input variable. In addition to the weight matrix, scholars also use multiple linear regression (MLR) to explain the significance of input variables, taking the significance output of MLR as the input of neural networks [18-20]. This method can also identify the direction of parameter influence (positive correlation or negative correlation), achieving satisfactory results based on linear and additive correlation.

Therefore, this paper uses MATLAB to construct a BR-BPNN. The average relative impact value (ARIV) is proposed as a quantitative index to evaluate the influence degree of various parameters related to fatigue life. It is verified through the comparison with the weight equation and MLR method. Based on the data from literature [21-24], the BR-BPNN with satisfactory generalization capability for concrete flexural fatigue is obtained and then applied to predict flexural fatigue life curves under various parameters. Finally, to investigate whether a significant discrepancy exists between fatigue properties un-

Preprints (www.preprints.org) | NOT PEER-REVIEWED | Posted: 17 May 2022 doi:10.20944/preprints202205.0232.v1

der different loading conditions [25], the fatigue life of plain concrete in splitting tension, axial tension, and flexure loading is analyzed through BR-BPNN.

2. Materials and Methods

2.1. Data Collection and Preprocessing

In fatigue experiments, the recordable parameters mainly include R, Smax, P, *f*, water-cement ratio (W/C), sand-cement ratio (S/C), and gravel-cement ratio (G/C), as shown in Table 1.

A dataset containing 27**4** data points is obtained from concrete flexural fatigue experiments in the literature [21-24]. The data in the literature [21-23] are randomly divided in a ratio of 8:2, obtaining 170 training data points and 44 test data points to guarantee the network accuracy. The remaining 60 data points in the literature [24] are reserved to verify the generalization capability further.

Table 1. Flexural fatigue experimental data.

Purpose	Reference	Smax	R	*f*(MPa)	W/C	S/C	G/C	Equations of S-N Curves
Network accuracy	Shi et al. [21]	0.65~0.9	0.08, 0.2, 0.5	6.08	0.45	1.18	2.74	(1) $\lg S = 0.01069 - 0.04093(1-R)\lg N$ (2) $S = 0.9860 - 0.06919\ (1-R)\ \lg N$
	Zheng [22]	0.65~0.9	0.1	7.65	0.35	1.47	2.40	(3) $S = 1.04808 - 0.06731\lg N$
	Wu et al. [23]	0.625~0.9	0.1~0.5	5.1	0.45	1.40	3.27	(4) $\lg S = 0.002 - 0.0408(1-R)\lg N$
Generalization capability	Li et al. [24]	0.6~0.9	0.1	7.68	0.40	1.16	2.47	(5) $\lg S = 0.0483 - 0.0426\lg N$ (6) $\lg S = 0.0089 - 0.0299\lg N \quad S \geq 0.78$ $\lg S = 0.0888 - 0.0504\lg N \quad S \leq 0.78$

When an artificial neural network is used for mutual prediction between flexural, splitting, and axial tension fatigue, additional 90 sets of experimental data are collected from concrete tensile fatigue literature [26-29], as shown in Table 2.

Table 2. Tensile fatigue experimental data.

Loading Type	Reference	Smin	Smax	*f*(MPa)
Splitting tension	Lu et al. [26]	0.15	0.7~0.85	2.63
Axial tension	Song et al. [27]	0, 0.15, 0.3	0.65~0.85	2.45
	Meng [28]	0.22, 0.27	0.75~0.85	2.69
	Wang [29]	0.1	0.7~0.9	3.06

In order to improve the convergence rate of the network and avoid the deviation adjustment of weight caused by dimensional differences [30], the normalization is used for data preprocessing. The scale transformation of original data is conducted according to Eqn. (1), which is realized by [y, ps] = mapminmax (x, $y_{\min}$, $y_{\max}$) in MATLAB, where ps represents the mapping relationship; x and y are the data before and after normalization; $y_{\max}$, $y_{\min}$ is the maximum and minimum of normalized boundary, respectively; $x_{\max}$, $x_{\min}$ is the maximum and minimum of input before normalization, respectively.

$$y = \frac{(y_{\max} - y_{\min}) \times (x - x_{\min})}{(x_{\max} - x_{\min})} + y_{\min} \tag{1}$$

The output needs to be returned to the original order of magnitude for practical application of the predicted results. Therefore, the anti-normalization is performed according to Eqn. (2), which is realized by x = mapminmax ('reverse', y, ps) in MATLAB.

Preprints (www.preprints.org) | NOT PEER-REVIEWED | Posted: 17 May 2022 doi:10.20944/preprints202205.0232.v1

$$x = \frac{(y - y_{\min}) \times (x_{\max} - x_{\min})}{(y_{\max} - y_{\min})} + x_{\min} \tag{2}$$

2.2 Basic Principle of Backpropagation Neural Network

BPNN, a multi-layer feedforward network trained by the error backpropagation algorithm, can classify arbitrarily complex patterns and map nonlinear multi-dimensional functions [31]. Its essence is to calculate the error through the forward transmission of function signal among neurons and then backpropagate the error signal to correct the weight and bias of the network, repeatedly iterating until the loss function is minimized.

The topological structure of the L-layer BPNN is shown in Figure 2. The network includes the input layer (layer 1), the hidden layers (layer 2~L-1), and the output layer (layer L), each layer consisting of several neurons [32]. $\vec{X} = [x_1, x_2, ...x_i]$ represents input vector and $\vec{O} = [o_1, o_2, ...o_k]$ represents output vector. $w_{ij}^{(l)}$ is the connection weight between the ith neuron in layer l-1 and the jth neuron in layer l; $b_j^{(l)}$ is the bias of the jth neuron in layer l, and $\varphi^{(l)}(\bullet)$ represents the activation function of layer l neurons. The input and output of neurons in hidden layer l are $V^{(l)} = [v_1^{(l)}, v_2^{(l)}, ...v_j^{(l)}]$ and $\boldsymbol{H}^{(l)} = [h_1^{(l)}, h_2^{(l)}, ...h_j^{(l)}]$, respectively. $v_j^{(l)} = \sum_{i=1}^{I} w_{ij}^{(l)} h_i^{(l-1)} + b_j^{(l)}$, where I is the number of neurons in layer l-1 and $h_j^l = \varphi^l(v_j^{(l)})$.

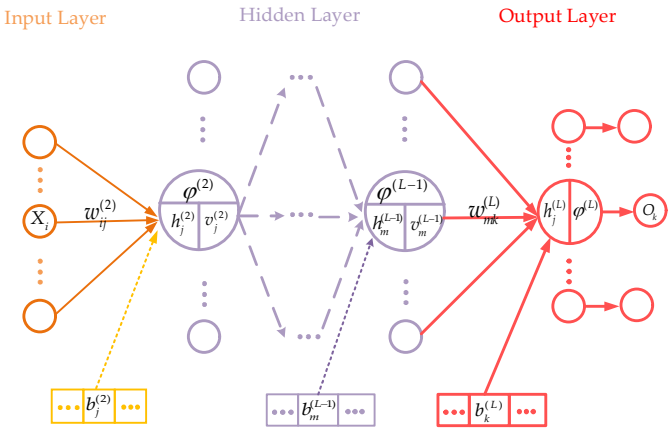

Figure 2. Topological structure of BPNN.

Suppose that the target output of the n-th training sample is $\vec{T} = [t_{1n}, t_{2n}, ...t_{kn}]$, the loss function is measured by mean square error (MSE): $E_D = \frac{1}{2N} \sum_{n=1}^{N} \sum_{k=1}^{K} (t_{kn} - o_{kn})^2$. The weight and bias are revised through the backpropagation of errors until the loss function is minimized through $w_{ij}^{(l)} = w_{ij}^{(l)} - \eta \frac{\partial E_D}{\partial w_{ij}^{(l)}}$ and $b_i^{(l)} = b_i^{(l)} - \eta \frac{\partial E_D}{\partial b_i^{(l)}}$, where η is the learning rate of backpropagation [33].

The classical BPNN with solid learning ability can achieve arbitrary fitting accuracy within the training samples [34]. However, the generalization capability of the network depends considerably on the number of neurons in the hidden layers. When the number of training samples is limited and the number of hidden layer neurons is vast, the model could produce a poor mapping effect on non-training samples. This phenomenon is called "overfitting"; the model exhibits high training accuracy but low prediction accura-

Preprints (www.preprints.org) | NOT PEER-REVIEWED | Posted: 17 May 2022 doi:10.20944/preprints202205.0232.v1

cy [35]. Therefore, achieving a good generalization capability of the BPNN is an essential research issue. A theoretical formula to determine the optimal number of hidden layer neurons has not yet been proposed. By trial and error, this paper finds out the optimal neuron number from the range of values suggested by an empirical equation, as represented in Eqn. (3):

$$m = \sqrt{i + k} + \lambda \tag{3}$$

where i is the number of neurons in the input layer, k is the number of neurons in the output layer, and λ is a constant between 1 and 10.

2.3 Bayesian Regularization

A network with a smaller weight or bias can obtain a smoother response, which is utilized by regularization to improve the generalization capability of the BPNN effectively [36], adding a penalty term to the target problem to limit its complexity. The L2 penalty term related to the weight is generally added to the loss function in the form of ridge regression [14].

The improved loss function is shown in Eqn. (4).

$$E(w) = \beta E_D + \alpha E_w = \frac{\beta}{2N}\sum_{n=1}^{N}\sum_{k=1}^{K}(t_{kn} - o_{kn})^2 + \frac{\alpha}{2M}\sum_{m=1}^{M} w^2 \tag{4}$$

where α and β are the regularization parameters, E_w is the penalty term of the loss function, and M is the number of connection weights.

Weight is modified as Eqn. (5). When updating the gradient to realize weight decay, the weight is multiplied by a constant coefficient less than 1.

$$w_{ij}^{(l)} = w_{ij}^{(l)} - \eta\frac{\partial E(w)}{\partial w_{ij}^{(l)}} = (1 - \eta\alpha)w_{ij}^{(l)} - \eta\beta\frac{\partial E_D}{\partial w_{ij}^{(l)}}, \tag{5}$$

α, β dramatically affects the distribution of weight and bias. When $\beta >> \alpha$, the decrease of training error cannot guarantee the generalization capability, as in the classical BPNN. Conversely, when $\beta << \alpha$, the attenuation of network scale and the smoother output is prone to cause "underfitting". This paper used the Bayesian computing framework to adaptively modify α and β, which reduced the training error and optimizes the network structure. The Bayesian technique can be expressed as in Eqn. (6):

$$\text{Posterior Probability} = \frac{\text{Likelihood Function} \times \text{Prior Probability}}{\text{Normalization Factor}} \tag{6}$$

It assumes that the likelihood function and priori probability satisfy the Gaussian distribution. Based on maximizing posterior probability, the L-M algorithm is used to solve the minimum of loss function $E(w_{opt})$. Then, the regularization parameters are further adjusted with the same idea through the Hessian matrix $\boldsymbol{H}$ at the minimum point w_{opt} to re-verify the accuracy of the loss function [14].

The following equations are obtained from the Bayesian technique [36], where γ is the number of valid parameters that reduce loss function in the network.

$$\alpha_{opt} = \frac{\gamma}{2E_w(w_{opt})}, \quad \beta_{opt} = \frac{N - \gamma}{2E_D(w_{opt})} \tag{6}$$

$$\gamma = M - 2\alpha tr(\mathbf{H}^{-1}(w_{opt})) \tag{7}$$

$$\mathbf{H} = \beta\nabla^2 E_D(w_{opt}) + \alpha\nabla^2 E_w(w_{opt}) \tag{8}$$

Preprints (www.preprints.org) | NOT PEER-REVIEWED | Posted: 17 May 2022 doi:10.20944/preprints202205.0232.v1

The learning steps of BR-BPNN are shown in Figure 3, which is realized by training function trainbr in MATLAB.

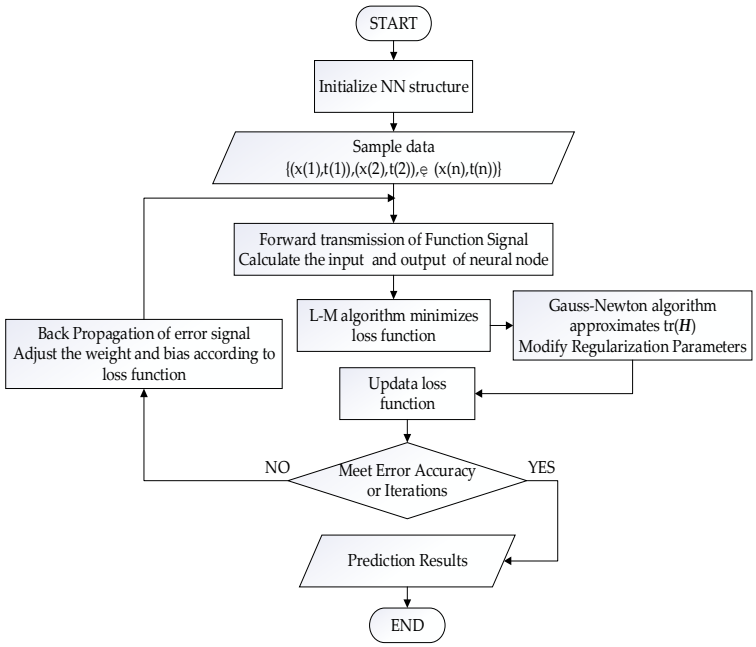

Figure 3. Learning flow chart of BR-BPNN.

2.4 Average Relative Impact Value (ARIV)

The correlation between output and input significantly affects the training quality of the network [17], while a coupling effect might exist among the parameters shown in Table 1. In order to determine the variables with significant effects and avoid model complexity induced by noise parameters, ARIV is used to determine the influence of input on output, whose symbol represents the relevant direction and the absolute value represents the relative importance.

Firstly, an original input variable, including i samples, is increased or reduced by 10% to derive two new data sets $\boldsymbol{X_1} = \{X_{11}, X_{12}, ...X_{1i}\}$ and $\boldsymbol{X_2} = \{X_{21}, X_{22}, ...X_{2i}\}$, where X_{1i} and X_{2i} represent the data set formed by a 10% increase or decrease of the i^{th} sample in this variable, respectively. Then the BR-BPNN trained by the original training sample predicts the other two data sets, and the corresponding prediction results are $\boldsymbol{O_1} = \{O_{11}, O_{12}, ...O_{1i}\}$ and $\boldsymbol{O_2} = \{O_{21}, O_{22}, ...O_{2i}\}$. The ratio of the difference between $\boldsymbol{O_1}$ and $\boldsymbol{O_2}$ to the original output $\boldsymbol{O}$ is defined as the relative impact value matrix (**RIVM**). RIVM is finally averaged according to the number of samples to obtain the ARIV of each input parameter, as shown in Eqns. (9-10).

$$\mathbf{RIVM} = \frac{\mathbf{O_1} - \mathbf{O_2}}{\mathbf{O}} \tag{9}$$

$$ARIV = avg(\mathbf{RIVM}) \tag{10}$$

2.5 Weight Equation

The weight matrix of a neural network can evaluate the relative importance of each input variable to the output variable [37]. For a three-layer BPNN which can complete the infinite approximation to any continuous function (in the closed interval) [38] and realize the function mapping from any input to output, Garson proposed an equation to calculate the influence weight of each input variable based on the weight matrix [15].

 doi:10.20944/preprints202205.0232.v1

This paper also utilizes the Garson's connection weight division equation [15] to evaluate the influence weight of input variables, as shown in Eqn. (11).

$$I_{jn} = \frac{\sum_{m=1}^{N_h}((|w_{jm}^{ih}| / \sum_{k=1}^{N_i}|w_{km}^{ih}|) \times |w_{mn}^{ho}|)}{\sum_{k=1}^{N_i}\left\{\sum_{m=1}^{N_h}((|w_{jm}^{ih}| / \sum_{k=1}^{N_i}|w_{km}^{ih}|) \times |w_{mn}^{ho}|)\right\}} \quad (11)$$

where I_{jn} is the influence weight of the j^{th} input parameter on the n^{th} output neuron. N_i, N_h is the number of input and hidden layer neurons, respectively; w^{ih}, w^{ho} is the connection weights from the input layer to the hidden layer and from the hidden layer to the output layer, respectively.

2.6 Multiple Linear Regression (MLR)

Multiple linear regression studies the explanatory relationship between independent and dependent variables reflected through regression equations [38]. Suppose that the random variable (y) changes with independent variables (x_k), and the linear regression relationship is represented in Eqn. (12).

$$y = \beta_0 + \beta_1 x_1 + \beta_2 x_2 + \bullet\bullet\bullet + \beta_k x_k + \varepsilon \quad (12)$$

where β_0 represents regression constant; $\beta_1 - \beta_k$ are the partial regression coefficients, representing the influence degree of independent variable on dependent variable; ε is standard estimation error.

After constructing the regression equation, its goodness of fit and statistical significance must be verified. Some good-fit indicators of the linear relationship of regression equation include: the adjusted coefficient of determination (Adjusted R^2) evaluates how much the independent variables can explain the variation of the dependent variable, the standard error of the estimates (SEE) indicates the degree of relative deviation between the actual value and the estimated value, F change is the constructed statistic to test the significance of the whole regression model, and Sig. F change is the probability corresponding to the F statistic.

The overall significance of the regression model does not guarantee the same for each independent variable. In order to extract significant variables to optimize the model structure, further significance testing of the regression coefficient is required. The partial regression coefficient (B) and its standard errors (Std.error) indicate the effect of independent variables on dependent variables. The magnitude of B represents the degree of influence, and the sign of B represents the direction of correlation. In addition, to judge the contribution of independent variables to the variation of dependent variables, the *T* test is used to test whether the probability corresponding to the t-statistic is equal to 0, where the t-statistic is constructed as $t = \frac{B}{Std.error}$. The tolerance (Tol) and variance inflation factor (VIF) are indexes of multicollinearity diagnosis, and it is generally believed that linear correlations probably exist between independent variables when Tol<0.1 or VIF>10.

3. Results and Discussion

3.1. Selection of Hyperparameter and Function

Learning rate affects step adjustment of the loss function. A smaller value will lead to a slower convergence rate and more extended network response time. However, if it is too large, the neural network will converge too quickly, and it could easily miss the globally optimal solution [39]. In this study, the learning rate was set to 0.01. Since the error tolerance parameter limits the neural network's weights to avoid falling into a local

Preprints (www.preprints.org) | NOT PEER-REVIEWED | Posted: 17 May 2022 doi:10.20944/preprints202205.0232.v1

optimum during the training process, the allowable error was set to 1e-6. The maximum number of iterations was set to 10,000, considering the network's excellent computing power. We took the default values in the MATLAB toolkit for the rest of the parameters.

The prediction effect of BR-BPNN depends on the selection of various functions. The activation function that must be continuously differentiable plays a nonlinear transformation role in the input and output [40], transforming the input of an infinite field into an output within a specified range. The learning function returns the correction value of weight and bias in each layer, considering the minimization of local errors. The training function realizes the output of the training records and calls the learning function during the training process to correct the connection weight and bias [41]. The training is terminated when the number of iterations or the calculation error of the loss function satisfies the preset value, considering the minimization of the global error.

This paper exhaustively conducts a combined trial of various functions in the algorithm. The optimal combination of activation function and learning function is selected based on the minimum MSE of the training result. The influence of function combinations on the results is shown in Figure 4.

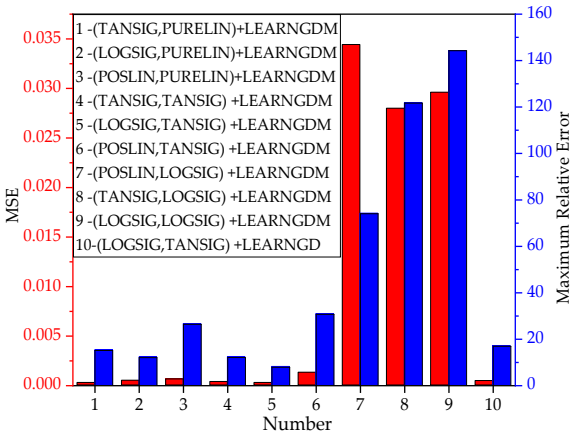

Figure 4. Influence of function combinations on training results.

Notes: 1~10 represents the combination number. The legend describes the combination mode according to activation function (the first for hidden layer, the second for output layer) + learning function. TANSIG is the hyperbolic tangent function; LOGSIG is the Sigmoid function; POSLIN is the positive linear function; PURELIN is the linear transfer function. LEARNGDM is the gradient descent momentum learning function; LEARNGD is the gradient descent learning function.

As seen from Figure 4, the No. 5 network structure (LOGSIG + TANSIG + LEARNGDM) has the lowest error performance with an MSE of 0.00024 and a maximum relative error of 7.89%. The final function combination is shown in Table 3.

Preprints (www.preprints.org) | NOT PEER-REVIEWED | Posted: 17 May 2022 doi:10.20944/preprints202205.0232.v1

Table 3. Selection of BR-BPNN functions.

Activation Function		Learning Function	Training Function	Performance Function
Hidden Layer	Output Layer			
LOGSIG	TANSIG	LEARNGDM	TRAINBR	MSE

3.2. Determination of the Neurons

The fatigue life N is used in the output layer to reflect the fatigue performance of concrete.

In order to obtain the influence effect of each variable, this paper analyzes the changes of the ARIV after ten times of random network training, as shown in Figure 5.

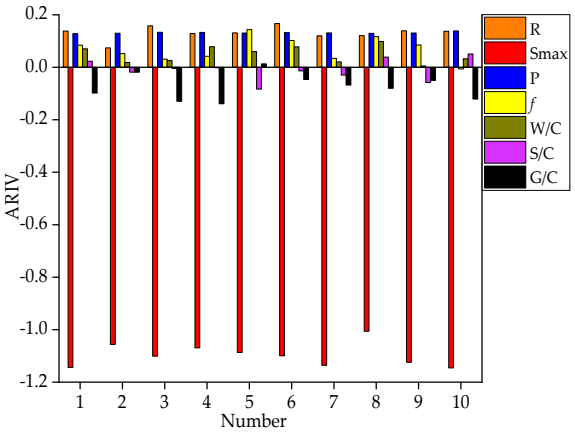

Figure 5. ARIV under 10 random training networks.

It can be seen from Figure 5 that the correlations reflected by ARIV of the R, Smax, P, and *f* are relatively consistent. While R, P, and *f* are proportional to fatigue life, Smax is inversely proportional to fatigue life. The most considerable absolute value of ARIV indicates that Smax has the most significant effect. The randomness of the initial weight and bias results in different prediction effects after multiple network training [16], so the ARIV is not constant. The ARIV of W/C, S/C, and G/C fails to show a consistent correlation, thus regarded as noise parameters. Therefore, the input layer neurons comprise four parameters: Smax, R, P, and *f*.

Ten network structures have been constructed for the range of hidden layer neurons determined by Eqn. (3). The correlation coefficients of network training and generalization under these ten network structures are shown in Figure 6. The final BR-BPNN then predicts fatigue life for tests conducted in the literature [24], and the generalization effect is shown in Figure 7.

Preprints (www.preprints.org) | NOT PEER-REVIEWED | Posted: 17 May 2022 doi:10.20944/preprints202205.0232.v1

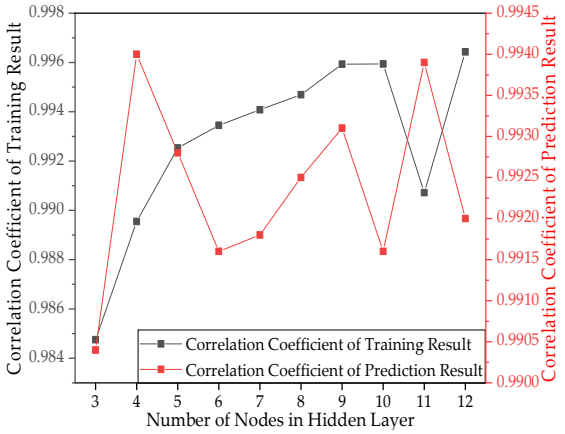

Figure 6. Correlation coefficients under different network structures.

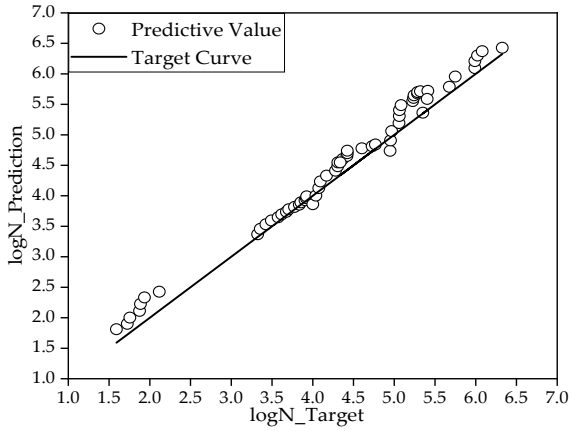

Figure 7. Generalization effect of BR-BPNN.

It is analyzed in Figure 6 that the correlation coefficient of the dataset for network training is 0.9959 (left axis) and that for generalization is 0.9931 (right axis) when the number of hidden layer neurons is 9, both of which show a strong correlation. This paper thus constructs the final BR-BPNN with nine hidden neurons, which demonstrates high correlation coefficients in both the training and generalization stages.

Figure 7 shows that the prediction coincides with the target curve, the MSE between the target value and the predicted value is 0.0482, and the correlation coefficient R is 0.9931. Therefore, the BR-BPNN model provides reliable generalization capability for the following direct applications to S-N curves prediction.

3.3. Feasibility Analysis of ARIV

The correlation between the input parameters and fatigue life was analyzed in Section 3.2 for random training networks. To reflect the influence degree of input parameters in more depth, the final BR-BPNN is used to re-analyze the ARIV of Smax, R, P, and *f*, and the results are shown in Table 4.

Preprints (www.preprints.org) | NOT PEER-REVIEWED | Posted: 17 May 2022 doi:10.20944/preprints202205.0232.v1

Table 4. ARIV analysis of input parameters for the final BR-BPNN.

Input Parameter	Analysis Result of ARIV
R	0.143
Smax	-0.871
P	0.122
f	0.116

It can be seen from Table 4 that the correlation between various input parameters and fatigue life is consistent with previous conclusions. The maximum stress level affects the fatigue life negatively; stress ratio, failure probability, and static strength are positively correlated with fatigue life. The absolute value of ARIV shows that Smax has the most significant effect on fatigue life, followed by R, P, and *f*. In this section, ARIV results are further verified by SPSS regression analysis and weight equation to accurately reveal the importance rank of input variables.

3.3.1. Verification by Weight Equation

Table 5 lists the value of 45 connection weights of the final BR-BPNN. w^{ih} comprises 36 connection weights from 4 input parameters to 9 neurons in the hidden layer, and w^{ho} comprises nine weights from the nine hidden layer neurons to the one output parameter of fatigue life.

Table 5. Connection weights of the BR-BPNN.

Weight		Neuron 1	Neuron 2	Neuron 3	Neuron 4	Neuron 5	Neuron 6	Neuron 7	Neuron 8	Neuron 9
w^{ih}	R	-2.466	0.241	-2.254	3.662	-2.485	-1.207	2.636	0.331	0.533
	S_{max}	-2.447	2.019	-3.015	-5.607	1.485	1.878	0.187	2.564	-3.537
	P	0.459	1.055	-0.278	0.973	-0.903	0.818	2.046	-0.280	0.818
	f	0.288	-1.000	-0.041	-1.023	0.272	0.263	-1.974	0.537	0.817
w^{ho}		-2.866	-1.634	-2.143	3.628	2.243	1.968	-0.822	-3.570	3.853

The influence weights of R, Smax, P, and *f* calculated from Eqn. (11) are 0.265, 0.501, 0.128 and 0.106, respectively. Therefore, it is concluded that the maximum stress level has the greatest influence on fatigue life, followed by stress ratio, failure probability, and static strength, which is consistent with the results from ARIV analysis.

3.3.2. Verification by SPSS Regression Analysis

Based on the correlation conclusions from Section 3.3.1 and the MLR equation in Section 2.6, three regression models are built, and the analysis results are shown in Table 6 and Figure 8. The difference between these models is primarily about whether to include the mix design parameters as independent variables.

Table 6. Summary of analysis results from MLR models.

Model	Dependent Variables	Independent Variables	Removed Variables	Adjusted R^2	SEE	F Change	Sig. F Change
1	lgN	Smax, R, P, *f*	/	0.931	0.05599	923.723	0.000
2		W/C, S/C, G/C	/	0.047	0.20832	5.453	0.001
3		Smax, R, P, *f* S/C, G/C	W/C	0.937	0.05371	673.596	0.000

It can be seen from Table 6 that all three models show a significance of less than 0.05, indicating that at least one factor of the regression model has a significant impact on fatigue life, which is statistically significant. Model 1 has a desirable fitting effect with an adjusted coefficient of determination of 0.931, indicating that Smax, R, P, and *f* can explain 93.1% variation in fatigue life. The goodness of fit for model 2 is poor, and W/C, S/C, and G/C could only account for a 4.7% variation in fatigue life. Introducing some

Preprints (www.preprints.org) | NOT PEER-REVIEWED | Posted: 17 May 2022 doi:10.20944/preprints202205.0232.v1

mixture ratio variables into model 3, the coefficient of determination only increases by 0.6%, compared with model 1, and SSE only reduces by 4%, further demonstrating that the mixture ratio has little effect on fatigue life.

Figure 8 shows the T-test results of partial regression coefficients. As shown in Figure 8(a), the significance value for all input parameters is less than 0.05, indicating that each of the four parameters (Smax, R, P, *f*) significantly affects fatigue life. In Figure 8(b), B's positive and negative display indicates that Smax has a negative impact, while R, P, and *f* have a positive impact. Since B_{Smax} = -0.873, B_R = 0.262, B_P =0.102, B_f = 0.067, the degree of influence of each parameter is: Smax > R > P > *f*. These results are also consistent with those from ARIV and weight equation analysis.

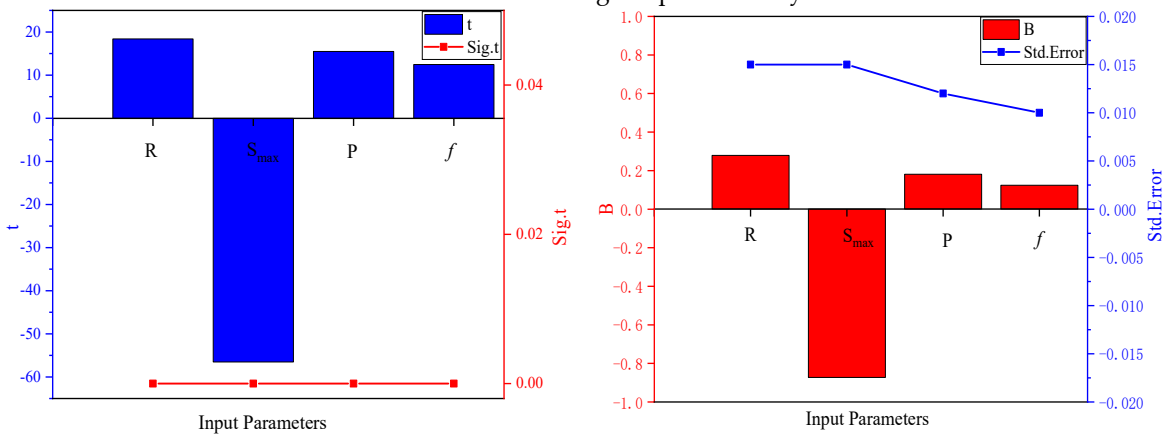

(**a**) (**b**)

Figure 8. Analysis results from T test: (**a**) T statistic and its significance; (**b**) Partial regression coefficient and its Std.error.

3.3.3. Comparison between Various Methods

ARIV analysis, weight equation analysis, and SPSS regression analysis show a consistent observation, which verifies the correctness of the final BR-BPNN. It also confirms the feasibility of ARIV in determining the correlation between inputs and outputs and the relative importance of various input parameters affecting fatigue life. However, whether ARIV is more practical than the other two methods needs further exploration of the advantages and disadvantages of the three methods in multi-parameter significance analysis.

The weight equation analysis evaluates the relative importance of the input parameters, which thoroughly explains the structural significance of the weight matrix in the neural network. As intuitive and concise as the method is, Eqn. (11) is only valid for the three-layer neural network, and the equation's operation with absolute values cannot show a positive or negative correlation between input parameters and fatigue life.

The mathematical meaning of SPSS MLR analysis is clear, and the influence of input parameters on fatigue life can be evaluated from the aspects of correlation and importance. However, this method assumes a linear fit of the regression equation without considering other types of relationships. It cannot reflect the actual mapping relationship well when the noise factor is included, which can be considered a limitation [42], as shown in Table 7. The collinearity statistics of *f* and G/C in Model 2 show that the model has multicollinearity. Then, the significance test of the independent variables and the model prediction function become meaningless.

Preprints (www.preprints.org) | NOT PEER-REVIEWED | Posted: 17 May 2022 doi:10.20944/preprints202205.0232.v1

Table 7. Regression coefficient analysis of Model 2.

Model	Independent Variables	Std.error	t	Sig.t	Collinear Analysis	
					Tol	VIF
2	R	0.015	19.235	0.000	0.485	2.062
	Smax	0.015	-57.089	0.000	0.634	1.577
	P	0.011	16.150	0.000	1.000	1.000
	f	0.030	-0.419	0.676	0.063	15.910
	S/C	0.009	3.018	0.003	0.769	1.301
	G/C	0.032	-4.876	0.000	0.062	16.108

Although ARIV analysis of a neural network is strongly model-dependent, it can deal with nonlinear relationships and could preliminarily screen out the noise variables with insignificant effects through trial calculation. It also helps to construct the optimal network, a feedback mechanism to evaluate the correlation between the input and output parameters and the relative importance of various input parameters. Therefore, compared with weight equation analysis and SPSS regression analysis, ARIV analysis has a broader scope of application, and it is recommended for future variable effect analysis.

3.4. S-N Curves Predicted by BR-BPNN

Based on experimental results, the conventional research on flexural fatigue of concrete is to fit maximum stress level versus fatigue life equation according to a failure probability of about 50%. The experimental data and S-N curves from various literature are shown in Figure 9.

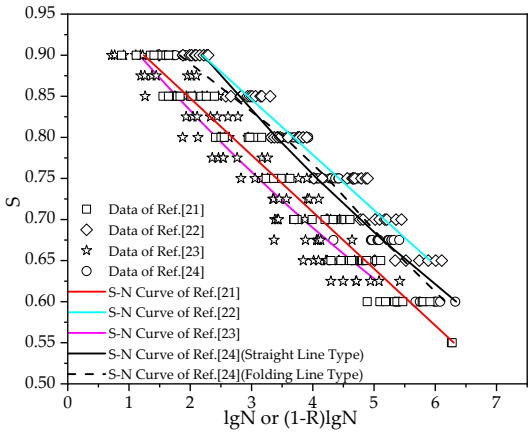

Figure 9. Test data and S-N curve from literature.

Because fatigue tests are generally time-consuming and expensive, the number of specimens in individual literature is limited, as shown in Figure 9. Therefore, it is desirable to combine them to obtain more accurate concrete fatigue life prediction under various stress states and guarantee rates.

This paper utilizes the generalization capability of BR-BPNN to predict concrete fatigue life in different states by giving different values of Smax, R, P, and *f*. In theory, the possible combinations of parameters are infinite. For practical demonstration, considering the input data characteristics for network training, the following text only shows the generalization effect when R=0.1, 0.2, 0.5; *f*=5, 6, 7MPa; P=5%, 50%, 95% for concrete flexural fatigue.

3.4.1. S-N Curve under 50% Guarantee Rate

Preprints (www.preprints.org) | NOT PEER-REVIEWED | Posted: 17 May 2022 doi:10.20944/preprints202205.0232.v1

Figure 10 shows the S-N curves predicted by the BR-BPNN under the 50% guarantee rate for various combinations of *f* and R. Besides the generalization curves, experimental data points from literature are also shown in the figure, and different pieces of literature are distinguished by shape. At a specified *f*, to facilitate comparison between the generalization curve and the experimental data, both the data points and curve under the same R are assigned with a unified color, black for R=0.1, magenta for R=0.2, and red for R=0.5.

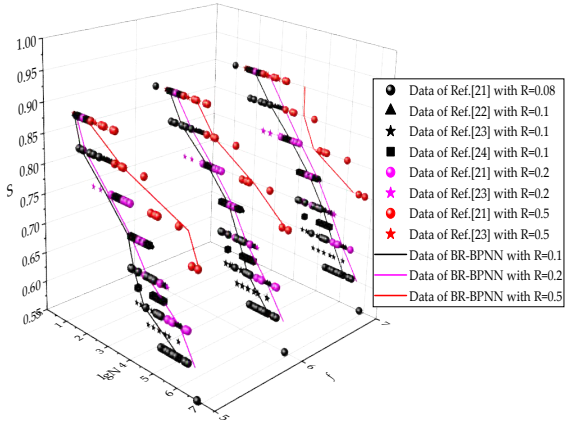

Figure 10. S-N curve under 50% guarantee rate predicted by BR-BPNN.

Conforming to the conclusions of Section 3.3, Figure 10 shows the relationship between fatigue life and its affecting factors vividly. It can be seen that the S-N curves generally agree well with the corresponding reference data. As S decreases, the fatigue life increases, although the relationship is not linear. Moreover, the fatigue life increases with an increase of R and *f*. Because few data points were available for R=0.5 in the network training dataset, the generalization effect of the S-N curve with R=0.5 is less satisfactory than that of R=0.1.

3.4.2. Probability Distribution of Fatigue Life

By changing P in BR-BPNN, reliability analysis could be conducted to evaluate the failure probability of concrete specimens under fatigue load. The S-N curve under the P of 5%, 50%, and 95% generalized by BR-BPNN is shown in Figure 11. Similarly, the prediction curves under the same P are assigned with a unified color, black for P=50%, magenta for P=5%, and red for P=95%.

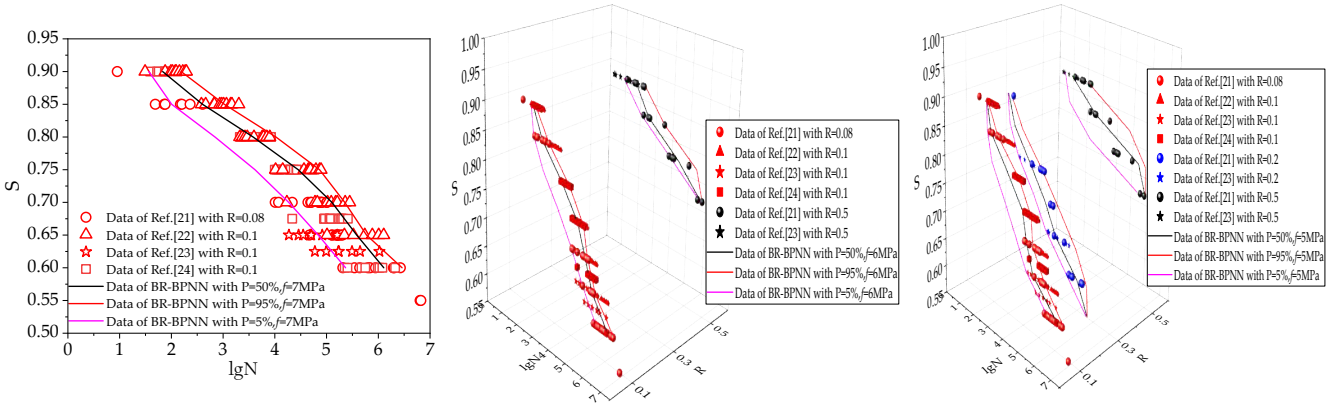

(**a**) (**b**) (c)

Figure 11. Probabilistic S-N curves predicted by BR-BPNN: (**a**) Probability analysis for *f* = 7MPa; (**b**) Probability analysis for *f* = 6MPa; (**c**) Probability analysis for *f* = 5MPa.

Preprints (www.preprints.org) | NOT PEER-REVIEWED | Posted: 17 May 2022 doi:10.20944/preprints202205.0232.v1

This section discusses the probability distribution of concrete flexural fatigue life. It can be seen from Figure 11 that the P of 5% curve represents a lower limit of fatigue life and the P of 95% curve is an upper limit of the fatigue life. The generalization capability of the network for the fatigue life probability analysis is optimal for *f*=5MPa. When *f*=6MPa, the fatigue life probability analysis at R=0.1 and 0.5 can be achieved. For *f*=7MPa, a satisfactory analysis can be obtained only at R=0.1.

As seen from the S-N curves, the predicted results are consistent with corresponding reference data when a strong correlation exists, which provides a comprehensive method to establish the probabilistic fatigue life curves from existing data.

3.5. Mutual Prediction of Flexural and Tensile Fatigue

Zhao et al. concluded that there were no significant discrepancies in fatigue properties for high-strength concrete under splitting tension, axial tension, and flexure [25]. To verify if the conclusion also applies to regular grade concrete, BR-BPNN is used to mutually predict flexure, splitting tension, and axial tension of fatigue life.

It should be noted that the axial/splitting tensile strength of concrete is less than the flexural strength. Since the model is only valid within the range of the input parameters, extrapolation beyond these ranges cannot be performed [11]. Suppose the static strength is considered an input parameter while training the network. In that case, it is foreseeable that the generalization effect of the network cannot be guaranteed due to the significant difference between the tensile strengths of different stress states, as shown in Figure 12.

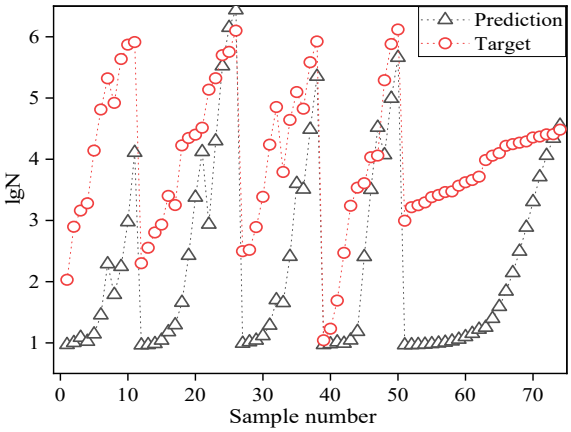

Figure 12. Prediction of tensile fatigue based on the 4-input parameters flexural fatigue network.

This section thus utilizes the three parameters of Smax, R, and P as inputs to construct a revised BR-BPNN. Due to the reduction of input parameters, the number of hidden neurons can be appropriately increased to improve the network complexity and ensure training accuracy. When 20 neurons in the hidden layer are selected through trial, the revised BR-BPNN provides a good prediction effect, as shown in Figure 13.

Preprints (www.preprints.org) | NOT PEER-REVIEWED | Posted: 17 May 2022 doi:10.20944/preprints202205.0232.v1

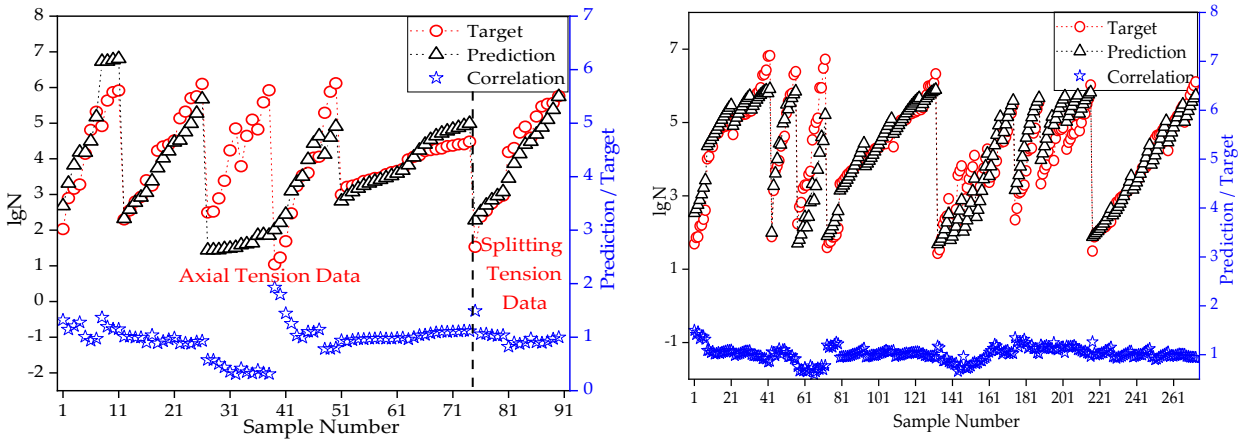

Figure 13. Mutual prediction of flexural and tensile fatigue life using BR-BPNN: (**a**) Prediction of tensile fatigue based on flexural fatigue network; (**b**) Prediction of flexural fatigue based on tensile fatigue network.

Figure 13(a) shows that the network based on flexural fatigue data approximates the fatigue life in the splitting state very well, and the correlation coefficient can reach 0.972. However, good feedback is obtained only in part of the data range for fatigue life prediction under axial tension. This range covers data points with Smin of 0.1 and 0.15, and Smax of 0.75~0.85, in which the correlation coefficient is 0.901.

Figure 13(b) shows that the network trained based on axial/splitting tension fatigue data has a good prediction effect on the flexural fatigue life. The overall correlation coefficient between the prediction and experimental results is 0.913.

In this section, a revised BR-BPNN is constructed to mutually predict the tensile and flexural fatigue data under certain circumstances. It verifies that a similar trend exists for fatigue lives between different tensile stress states; thus, to some extent, the experimental results of splitting tension, axial tension, and flexure could be combined in future analysis.

4. Conclusions

Considering fatigue life of concrete is affected by loading and material properties that are nonlinearly interwoven, this paper utilizes BR-BPNN to evaluate parameters affecting fatigue life and predict fatigue life under different experimental conditions. The analysis is based on an input dataset with 364 data points obtained from experiments reported in the literature, and we draw the following conclusions:

(1) The constructed ARIV approximates the internal logical relationship of each parameter through a non-explicit algorithm, resulting in an objective evaluation of the relative importance of parameters. In analyzing multiple variables directly affecting fatigue life, Smax is found to have the most significant impact on concrete fatigue life among the seven parameters considered, followed by R, P, and *f*. The mix ratio is regarded as the noise parameter. These findings are also verified by Garson's weight equation analysis and SPSS MLR analysis.

(2) The optimal BR-BPNN constructed in this paper is reliable in predicting the concrete flexural fatigue life. The correlation coefficient in the stage of network training can reach 0.9959. When verifying the generalization capability of the network, it still shows a strong correlation of 0.9931, indicating that the network has high accuracy in both the training and generalization stages.

(3) The BR-BPNN can predict concrete fatigue life for any acceptable level of failure probability. The S-N curves under the 5% and 95% failure probability could be practically taken as the lower and upper bound limits of concrete flexural fatigue life, which pro-

 doi:10.20944/preprints202205.0232.v1

vides a reference range of expectations when evaluating the fatigue performance of concrete subjected to fatigue loading.

(4) This paper verifies the compatibility of tensile fatigue tests on plain concrete under different stress states. The prediction of axial/splitting tensile fatigue life from a neural network based on a flexural tensile fatigue dataset shows applicability for all splitting tensile fatigue data and axial tensile fatigue data with Smin of 0.1 and 0.15 and Smax between 0.75 and 0.85. On the contrary, the overall correlation coefficient between predicted results and experimental values reaches 0.901 when predicting flexural fatigue life from the other two modes of tensile fatigue dataset.

(5) The most suitable BR-BPNN for different research problems might not be identical. When predicting concrete flexural tensile fatigue, the model with four input parameters (Smax, R, P, and *f*), one output parameter (N), and one hidden layer with nine neurons has the best performance. However, in the mutual prediction between flexural tension fatigue data and axial/splitting tension fatigue data, the optimal BR-BPNN consists of three input parameters (Smax, R, and P) and one hidden layer with 20 neurons.

By utilizing the valuable fatigue test data scattered in the literature, this paper demonstrates that BR-BPNN could predict fatigue life under various conditions. For practical applications of fatigue test program design and fatigue evaluation, BR-BPNN could replace part of the expensive and time-consuming fatigue experiment and play the role of an auxiliary test. However, BR-BPNN has high requirements on the number of samples in the data set for training. When sufficient sample data becomes available, more material parameters, more complex experimental conditions, and more types of concrete materials should be incorporated into the model for further analysis and future research.

Author Contributions: Conceptualization, Huating Chen and Yan Huang; Data curation, Zhenyu Sun and Zefeng Zhong; Formal analysis, Huating Chen and Zhenyu Sun; Funding acquisition, Huating Chen and Yan Huang; Investigation, Huating Chen and Zhenyu Sun; Methodology, Huating Chen, Zhenyu Sun and Zefeng Zhong; Project administration, Huating Chen and Yan Huang; Resources, Huating Chen and Yan Huang; Software, Zhenyu Sun and Zefeng Zhong; Supervision, Huating Chen and Yan Huang; Validation, Zhenyu Sun and Zefeng Zhong; Visualization, Zhenyu Sun; Writing – original draft, Huating Chen and Zhenyu Sun; Writing – review & editing, Huating Chen, Zhenyu Sun, Zefeng Zhong and Yan Huang. All authors have read and agreed to the published version of the manuscript.

Funding: This research was funded by the National Natural Science Foundation of China, grant number 51008006. The APC was funded by the open access program of Beijing University of Technology.

Data Availability Statement: Details of flexural fatigue experimental data (274 data points), tensile fatigue experimental data (90 data points), and the four-parameter BR-BPNN model presented in this study are available on request from the corresponding author. The data are not publicly available due to privacy.

Conflicts of Interest: The authors declare no conflict of interest. The funders had no role in the design of the study; in the collection, analyses, or interpretation of data; in the writing of the manuscript, or in the decision to publish the results.

List of Notations

$b_j^{(l)}$	bias of the jth neuron in layer l
f	static strength of concrete
$h_j^{(l)}$	output of jth neurons in hidden layer l
i	suggested number of neurons in the input layer
k	number of neurons in the output layer
m	number of neurons in the hidden layer
ps	mapping relationship

 doi:10.20944/preprints202205.0232.v1

t	conducted statistic
$w_{ij}^{(l)}$	connection weight between the i[th] neuron in layer l-1 and the j[th] neuron in layer l
w_{opt}	minimum point of loss function
x	data before normalization
$x_{\max}$	maximum value of input data before normalization
$x_{\min}$	minimum value of input data before normalization
y	data after normalization
$y_{\max}$	maximum boundary of data after normalization
$y_{\min}$	minimum boundary of data after normalization
ARIV	average relative impact value
B	partial regression coefficient
B_f	partial regression coefficient of static strength
B_P	partial regression coefficient of failure probability
B_R	partial regression coefficient of stress ratio
B_{Smax}	partial regression coefficient of maximum stress level
BPNN	backpropagation neural network
BR-BPNN	Bayesian regularized backpropagation neural network
E_D	loss function
$E(w)$	improved loss function
$E\left(w_{opt}\right)$	minimum of loss function
E_w	penalty term of the loss function
F change	constructed statistic
G/C	gravel-cement ratio
$\boldsymbol{H}$	Hessian matrix
$\boldsymbol{H}^{(l)}=[h_1^{(l)},h_2^{(l)},...h_j^{(l)}]$	output of neurons in hidden layer l
I	number of neurons in layer l-1
M	number of all connection weights
MLR	multiple linear regression
MSE	mean square error
N	number of stress cycles; number of training samples
$\boldsymbol{O_1}=\{O_{11},O_{12},...O_{1i}\}$	prediction results for data set X_1
$\boldsymbol{O_2}=\{O_{21},O_{22},...O_{2i}\}$	prediction results for data set X_2
$\vec{\boldsymbol{O}}=[o_1,o_2,...o_k]$	output vector
P	probability of fatigue failure
R	stress ratio, defined as minimum stress divided by maximum stress
R^2	coefficient of determination
RIVM	relative impact value matrix
S	stress level, defined as fatigue stress divided by f
S/C	sand-cement ratio
SEE	standard error of the estimates
Sig. F change	probability corresponding to the F statistic
Sig,t	probability corresponding to the t statistic
Smax	maximum stress level, defined as maximum fatigue stress divided by f
Smin	minimum stress level, defined as minimum fatigue stress divided by f
Std.error	standard errors
Tol	tolerance
$\vec{T}=[t_{1n},t_{2n},...t_{kn}]$	target output of the n-th training sample
$V^{(l)}=[v_1^{(l)},v_2^{(l)},...v_j^{(l)}]$	input of neurons in hidden layer l

 doi:10.20944/preprints202205.0232.v1

VIF	variance inflation factor
W/C	water-cement ratio
$\boldsymbol{X_1} = \{X_{11}, X_{12}, ...X_{1i}\}$	data set derived by increasing the original inputs by 10%
$\boldsymbol{X_2} = \{X_{21}, X_{22}, ...X_{2i}\}$	data set derived by decreasing the original inputs by 10%
$\vec{\boldsymbol{X}} = [x_1, x_2, ...x_i]$	input vector
α	regularization parameter
α_{opt}	improved regularization parameter
β	regularization parameter
β_{opt}	improved regularization parameter
β_0	regression constant
$\beta_1 - \beta_k$	partial regression coefficients
γ	number of valid parameters reducing MSE
$\varphi^{(l)}(\bullet)$	activation function of layer l neurons
η	learning rate of backpropagation
λ	constant between 1 and 10 for estimating m
ε	standard estimation error

References

1. Shen, J.; Liu, X.Y.; Wu, L. Fatigue performance of concrete with pre-cracks in tension-compression cycles. *Appl. Mech. Mater.* **2014**, 584-586, 1054-1061.
2. Zheng, J.; Xu, J.; Liu, C.; et al. Prediction of rubber fiber concrete strength using extreme learning machine. *Front. Mater.* **2020**, 582635.
3. Tepfers, R.; Kutti, T. Fatigue strength of plain, ordinary and lightweight concrete. *ACI J. Proc.* **1979**, 76, 5, 635-652.
4. Oh, B.H. Fatigue life distributions of concrete for various stress levels. *ACI Mater. J.* **1991**, 88, 2, 122-128.
5. Zhang, B. Effects of loading frequency and stress reversal on fatigue life of plain concrete. *Mag. Concr. Res.* **1996**, 48, 177, 361-375.
6. Chen, J.; Liu, Y.M. Fatigue modeling using neural networks: A comprehensive review. *Fatigue Fract. Eng. Mater. Struct.* **2022**, 4, 945-979.
7. Nowell, D.; Nowell, P.W. A machine learning approach to the prediction of fretting fatigue life. *Tribol. Int.* **2020**, 141, 105913.
8. Lu, P.Y.; Song, Y.P. Fatigue life estimation of concrete based on artificial neural network. *Ocean Eng.* **2001**, 19, 3, 72-76.
9. Peng, K.K.; Huang, P.Y; Guo, X.Y. Predication for Fatigue Lives of RC Beams Strengthened with CFL based on Neural Network Algorithm. In Proceedings of 2nd International Conference on Structural Condition Assessment, Monitoring and Improvement (SCAMI-2), Changsha, China, 19-21 November 2007; pp. 1152-1157.
10. Xiao, J.Q.; Ding, D.X.; Xu, G.; et al. Implication of portable artificial neural network and its practice on fatigue life estimation of concrete. *J. Univ. South China, Sci. Technol. Ed.* **2009**, 23, 1, 96-100.
11. Abambres, M.; Lantsoght E.O.L. ANN-based fatigue strength of concrete under compression. *Materials* **2019**, 12, 22, 3787.
12. Mohanty, R.; Verma, B.B.; Ray, P.K.; et al. Application of artificial neural network for fatigue life prediction under interspersed mode-I spike overload. *J. Test. Eval.* **2010**, 38, 177-187.
13. Yang, J.Y.; Kang, G.Z.; Liu, Y.J.; et al. A novel method of multiaxial fatigue life prediction based on deep learning. *Int. J. Fatigue* **2021**, 151, 106356.
14. Bezazi, A.; Pierce, S.G.; Worden, K. et al. Fatigue life prediction of sandwich composite materials under flexural tests using a Bayesian trained artificial neural network. *Int. J. Fatigue* **2007**, 29, 738-747.
15. Garson, G.D. Interpreting neural-network connection weights. *AI Expert* **1991**, 6, 46-51.
16. Li, X.; Zhang, W. Long-term fatigue damage assessment for a floating offshore wind turbine under realistic environmental conditions. *Renewable Energy* **2020**, 159, 570-584.
17. Lopes, T.A.P.; Ebecken, N.F.F. In-time fatigue monitoring using neural networks. *Mar. Struct.* **1997**, 10, 363-387.
18. Adamopoulos, S.; Karageorgos, A.; Rapti, E.; et al. Predicting the properties of corrugated base papers using multiple linear regression and artificial neural networks. *Drewno* **2016**, 59, 61-72.
19. Ausati, S; Amanollahi, J. Assessing the accuracy of ANFIS, EEMD-GRNN, PCR, and MLR models in predicting PM2.5. *Atmos. Environ.* **2016**, 142, 465-474.
20. Lin, L.H.; Lu, F.M.; Chang, Y.C. Prediction of protein content in rice using a near-infrared imaging system as a diagnostic technique. *Int. J. Agric. Biol.* **2019**, 12, 195–200.
21. Shi, X.P.; Yao, Z.K.; Li, H.; et al. Study on flexural fatigue behavior of cement concrete. *China Civ. Eng. J.* **1990,** (03), 11-22.
22. Zheng, K.R. *Effect of Mineral Admixtures on Fatigue Behavior of Concrete and Mechanism*; Southeast University: Nanjing, China, 2005.

23. Wu, Y.Q.; Gu, H.J.; Li, H.C. The S-P-N equation of concrete flexural tensile fatigue. *Concrete* **2005,** (01), 46-48.
24. Li, Y.Q.; Che H.M. A study on the cumulative damage to plain concrete due to flexural fatigue. *China Railw. Sci.* **1998**, 54-61.
25. Zhao, G.Y.; Wu, P.G.; Zhan W.W. The fatigue behaviour of high-strength concrete under tension cyclic loading. *China Civ. Eng. J.* **1993**, 13-19
26. Lu, P.Y.; Song, Y.P. Experimental investigation of fatigue behavior of concrete under cyclic tension loading at different temperatures. *Eng. Mech.* **2003,** (02), 80-86.
27. Song, Y.P.; Lu, P.Y. Study on the behavior concrete under axial tension-compression fatigue loading. *J. Build. Struct.* **2002**(04): 36-41.
28. Meng, X.H. *Experimental and Theoretical Research on Residual Strength of Concrete under Fatigue Loading*; Dalian University of Technology: Dalian, China, 2006.
29. Wang, Y.H. *Study on Mechanical Properties of Concrete under Axial Tension-Compression Fatigue Loading*; Dalian University of Technology: Dalian, China, 2010.
30. Liu, F.; Gong, H.; Cai, L.G.; et al. Prediction of ammunition storage reliability based on improved ant colony algorithm and BP neural network. *Complexity* **2019**, 5039097
31. Abiodun, O.I.; Jantan, A.; Omolara, A.E.; et al. State-of-the-art in artificial neural network applications: A survey. *Heliyon* **2018**, 4, e00938.
32. Kalayci, C.B.; Karagoz, S.; Karakas, Z. Soft computing methods for fatigue life estimation: A review of the current state and future trends. *Fatigue Fract. Eng. Mater. Struct.* **2020**, 43, 2763-2785.
33. Kazi, M.K.; Eljack, F.; Mahdi, E. Predictive ANN models for varying filler content for cotton Fiber/PVC composites based on experimental load displacement curves. *Compos. Struct.* **2020**, 254, 112885.
34. Bishop, C.M. *Neural Networks for Pattern Recognition*; Oxford University Press: Oxford, UK; 1996.
35. Mahamad, A.K.; Saon, S.; Hiyama, T. Predicting remaining useful life of rotating machinery based artificial neural network. *Comput. Math. Appl.* **2010**, 60, 1078-1087.
36. Foresee, F.D.; Hagan, M.T. Gauss-Newton Approximation to Bayesian Learning. In Proceedings of IEEE International Conference on Neural Networks (ICNN'97), Houston, TX, USA, 9-12 June 1997; pp. 1930-1935.
37. Aleboyeh, A.; Kasiri, M.B.; Olya, M.E. et al. Prediction of azo dye decolorization by UV/H2O2 using artificial neural networks. *Dyes Pigm.* **2008**, 77, 288-294.
38. Xu, X.; Sun, Z.; Wang, L. et al. A comparative study of customer complaint prediction model of time series, multiple linear regression and BP neural network. *J. Phys.: Conf. Ser.* **2019**, 1187, 052036.
39. Ebhota, V.C.; Srivastava, V.M. Performance analysis of learning rate parameter on prediction of signal power loss for network optimization and better generalization. *Wireless Pers. Commun.* **2021**, 118, 1111-1128.
40. Fathalla, E.; Tanaka, Y.; Maekawa, K. Remaining fatigue life assessment of in-service road bridge decks based upon artificial neural networks. *Eng. Struct.* **2018**, 171, 602-616.
41. Howard, D.; Mark, B.; Martin, H. *Neural Network Toolbox 5 User's Guide*; The MathWorks Inc.: Natick, MA, USA, 2004; pp. 198-263.
42. Sampaio, P.S.; Almeida, A.S.; Brites, C.M. Use of artificial neural network model for rice quality prediction based on grain physical parameters. *Foods* **2021**, 10, 3016.